THE JOURNAL OF PHYSICAL CHEMISTRY C

Article

pubs.acs.org/JPCC

# Synthesis and Characterization of the Nonlinear Optical Properties of Novel Hybrid Organic–Inorganic Semiconductor Lead Iodide Quantum Wells and Dots

I. Papagiannouli,[†,‡] E. Maratou,[§] I. Koutselas,*[,§] and S. Couris*[,†,‡]

[†]Department of Physics, University of Patras, 26504 Patras, Greece

[‡]Institute of Chemical Engineering and High Temperature Chemical Processes (ICE-HT), Foundation for Research and Technology-Hellas (FORTH), 26504 Patras, Greece

[§]Materials Science Department, University of Patras, 26504 Patras, Greece

**ABSTRACT:** Synthesis and characterization of the nonlinear optical properties of a class of semiconductors based on hybrid organic–inorganic two-dimensional semiconductors are being reported. A new simple synthetic route for the preparation and stabilization of lead iodide quantum dots (QD), based on $(PbI_6)^{4-}$ structural units, provided a variety of appropriate solutions of zero-dimensional (0D) and suspensions of two-dimensional (2D) hybrid organic–inorganic semiconductors. The third-order nonlinear optical properties of both semiconducting systems were studied by means of the Z-scan technique under visible (532 nm) and infrared (1064 nm), 35 ps and 4 ns laser excitation. The third-order susceptibility $\chi^{(3)}$ and second-order hyperpolarizability $\gamma$ were determined and are reported for the first time, showing gigantic enhancement in the case of the 2D material, reaching at least 5 orders of magnitude higher NLO response than that of the 0D material QDs, suggesting their potential for photonic and optoelectronic applications and devices.

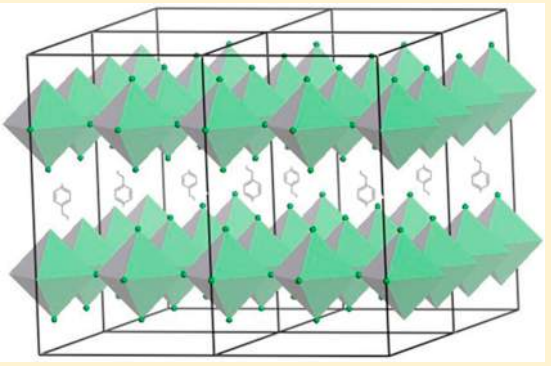

## 1. INTRODUCTION

During the past years, semiconductor-based nanosized entities in the form of plates, wires, and dots, with at least one of their spatial dimensions smaller than the material's exciton Bohr radius, have attracted significant attention due to their exciting physical, chemical, and optical properties and related potential applications. Their atomic size, chemical stability, high damage threshold, strongly manifested quantum confinement effects, and the capability to self-organize in various macroscopic structures position those as promising candidates for applications such as all optical switching,[1] laser media,[2] tunable optical filters,[3] and novel materials for integration in photovoltaic systems and sensors. In this respect, the synthesis and their physical properties have been extensively studied.[4−9] For example, the self-organization effects of these low-dimensional semiconductors (LD) or their basic units (i.e., zero-dimensional or 0D) such as their ability to form larger 0D units, one-dimensional (1D), two-dimensional (2D), or three-dimensional (3D) superlattices structures have led to an increasing interest for their linear and nonlinear optical (NLO) response.[10−20] A particularly interesting class of these LD materials is based on hybrid organic–inorganic semiconductors, where the organic part forms the inorganic part into various LD shapes and most of them are based in octahedral halogen-coordinated metal cations.[21] In that context, the NLO response of isolated quantum dots (QDs) is rather limited,[22−26] especially for hybrid organic–inorganic LD semiconductors. The most studied artificial semiconductors, regarding their NLO response, are $CdS_xSe_{1-x}$-based QDs, while less studied are LD systems based on $PbI_6$ or other metal halide units forming 0D, 1D, 2D, or other intermediate systems, which are all considered as perovskite-type materials.[21] However, no reports are available in the literature, to the authors' knowledge, regarding the NLO properties of the main structural unit of the previously named set of LD dimensional semiconductors, while only one work[19] is cited further for actual measurements of NLO properties of the LD hybrid quantum well material, similar to the one reported here. In this work, we focus on the study of the main block of $PbI_6$-based QDs, which are also the basic structural building block of a variety of LD systems in the form of 0D, 1D, 2D, and intermediate dimensionalities semiconductor systems, as well as on the 2D system in the form of suspensions. In that view, we report on a new synthetic route for creating and stabilizing $PbI_6$-based QD solutions in acetonitrile (AcN) as well as on measuring their NLO properties and compare them to those of suspensions of 2D hybrid LD materials in carbon tetrachloride ($CCl_4$). For the NLO investigation, the Z-scan has been used, while the optical

**Received:** September 26, 2013
**Revised:** January 13, 2014

   dx.doi.org/10.1021/jp409620w | J. Phys. Chem. C XXXX, XXX, XXX–XXX

Kerr effect (OKE) has been employed for the measurement of the nonlinearity and the temporal evolution of the 0D material under 532 nm, 35 ps laser pulses.

## 2. EXPERIMENTAL SECTION

**Chemicals.** 4-Fluorophenethylamine (abbreviated FpA, 98%), acetonitrile (CHROMASOLV Plus, for HPLC, ≥99.9%), hydriodic acid (ACS reagent, ≥47.0%), lead(II) iodide (99.999% trace metals basis), and carbon tetrachloride (CHROMASOLV, for HPLC) were obtained from Sigma-Aldrich.

**Synthesis.** The synthesis of the compounds reported and studied here, initially reported elsewhere,[27] is analogous to the hybrid organic−inorganic fluorophenethylamine (FpA)−tin iodide LD semiconductor reported by Mitzi et al.[28,29] Because of the investigation of the NLO properties, it is crucial that any effects and/or contribution arising from other structural material configuration, defects, or remaining solvent are to be excluded. For this, effort has been placed to avoid these problems by means of careful and simple synthetic methods. Thus, despite the multitude of synthetic routes, the reported synthesis of $(FpAH)_2PbI_4$ was performed in two specific steps in order to ensure that reference measurements are suitable for systematic exclusion of any unwanted effects in the nonlinearity of the final QD solutions.

Initially, 7.62 mmol of FpA was mixed at 48 °C in 5 mL of AcN and treated slowly with 7.62 mmol of HI. This solution has also been used as reference material, in measuring the NLO effects of the amine salt in the solvent environment of this synthesis (i.e., AcN/acid). A second solution of 3.8 mmol of $PbI_2$ in AcN was treated with 9.1 mmol of HI at 48 °C and was slowly added, under mixing, to the first solution, giving rise to a dark orange colored solution, whose assay strongly fluoresces in green, even under native room light, observable with the naked eye. Slow cooling gave rise to red-orange crystals, with an average size of about 1 mm, which can be redissolved and recrystallized in AcN for further usage. Chemical analysis of the crystals through energy-dispersive X-ray (EDS) measurements yielded the atomic ratio of I:Pb (i.e., 79.99:14.56), while elemental analysis has been solved, giving rise to an atomic ratio of N:C:H:Pb:I, i.e., 1:7.62:9.45:1:4). This system, as it is isomorphic to the one previously studied by Mitzi et al.[28,29] as well as to other similar systems,[30,31] is composed of alternating sheets of corner sharing lead iodide octahedrons, $(PbI_6)^{4-}$, and protonated positively charged organic molecules, i.e., $(FpAH)^+$, separating and connecting the inorganic sheets, as it is visually depicted in Scheme 1.

It must be noted that such a system is considered as an organic−inorganic hybrid 2D LD semiconductor. Also, in dilution its inorganic and organic constituents break into smaller units that are not, however, leading to the formation of lead iodide. In fact, these units are organic amine capped $PbI_6$ negatively charged octahedra. It is well-known that $PbI_2$ can exist in certain solvents, however, in quite small concentrations. Among these solvents, dimethylformamide, AcN, and $H_2O$ have been studied before[32−34] as to the extent of withholding nanosized species of lead iodide units, which are considered to be QDs, exhibiting pronounced blue-shifted absorption spectra with respect to the band gap of $PbI_2$. Depending on the choice of the solvent, it has been shown in these previous research works,[32−34] as far as relatively low concentration solutions are being discussed, that it is possible to generate rather monodispersed semiconducting species with specific absorption

**Scheme 1. Crystalline Structure of the Low-Dimensional (2D) Hybrid Organic Inorganic Semiconductor Composed of Alternating Inorganic and Organic Sheets, While the Inorganic Sheets Are Composed of Corner Sharing Octahedral, the Basic Unit of the 0D Solutions**

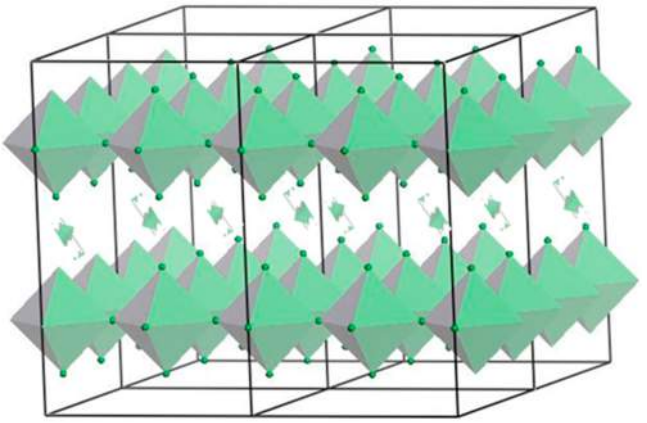

peaks in the UV region, which can be rather evident in solutions whose concentration varies within specified limits. In this work we have investigated solutions of lead iodide QDs. They have been prepared by diluting the $(FpAH)_2PbI_4$ in AcN, after it was degassed with $N_2$ for 6 h, where it is considered that QDs are being formed as the minimum-sized entity created by the 2D system and capped with amine salt molecules. The formation of the nanostructures in the AcN solution was verified by comparison of the characteristic UV peaks to the corresponding of the 2D material, where neither 3D nor 2D lead iodide UV peaks were detected in the solution, nor other unknown peaks. Dilution followed by evaporation of the solvent leads to the formation of the starting 2D material as before, with no traces of $PbI_2$ being formed, as it has been verified by XRD and optical measurements.

Also, solutions of quite high and low concentrations of QDs, as prepared before, lead to the same optical absorption spectra. In fact, the UV−vis absorption peaks in AcN are exactly the same as those of pure $PbI_2$ being diluted in AcN, but in this case the existence of the amine allows much larger concentrations and prohibits the solidification in $PbI_2$, which would be the case if no amine was being used at high QD concentrations. The reported 2D semiconductor's synthesis and subsequent analysis of the solution spectra are very important for the methodological understanding of the NLO effects of the QDs and the layered material itself.

In particular, the inorganic layer breakup could theoretically create a multitude of $Pb_xI_y$ species, all capped with the amine salt molecules. However, it is quite important to stress that the UV−vis absorption spectra exhibit a peak at about 360 nm, which is also appearing in the solid phase absorption peak of $(CH_3NH_3)_4PbI_6.4H_2O$,[30,31] which is composed of isolated octahedral $PbI_6$. Therefore, it is safe to conclude that the peak at 360 nm is due to the absorption by a specific lead iodide octahedron, while the breadth of any peak is due to any other species that has formed, as well as due to the interaction of the octahedrons through the amine salt. Thus, the resulting solutions being used here for NLO studies demonstrate the characteristic optical features of the basic building block of a large variety of LD semiconductors.


dx.doi.org/10.1021/jp409620w | J. Phys. Chem. C XXXX, XXX, XXX−XXX

The 2D hybrid organic−inorganic semiconductor was also dissolved at the concentration of 6.84 mg in 0.7754 g of AcN, while 33 $\mu$L of the resulting solution was slowly injected in 2 g of carbon tetrachloride under intense stirring, which creates a suspension, where the 2D material crystallizes in microdroplets of AcN within the $CCl_4$, as evidenced by the strong color change and relevant optical absorption spectra. Fast addition does not yield good quality 2D suspension of AcN in $CCl_4$ in the sense that the formed material is not in the form of 2D material but probably contains units of higher dimensionality.

**Methods.** X-ray powder diffraction (XRD) data were obtained from powdered polycrystalline samples on a Bruker D8 Advance diffractometer equipped with a LynxEyedetector and Ni-filtered Cu K$\alpha$ radiation. The scanning area covered the $2\theta$ interval 2°−80°, with a scanning angle step size of 0.015° and an integration time step of 17 s. Elemental analysis was performed in a Carlo−Erba model NA-1500. In addition, UV−vis spectra were recorded on a Hitachi U2800 spectrophotometer in the range of 200−800 nm, at a sampling step of 2 nm with 1.5 nm slits, using a combination of halogen and deuterium lamps as sources. The presented spectra were measured from thin films of spin-coated sample solutions on quartz, heated at 90 °C to remove solvent traces. The photoluminescence (PL) and photoluminescence excitation (PLE) spectra were obtained from solid pressed pellets or thin deposits on quartz plates, mounted in a Hitachi F-2500 FL spectrophotometer employing a xenon 150 W lamp and a R928 photomultiplier detector. The excitation and detection slits were set at 2.5 nm. The PLE and emission spectra have been corrected through the instrument supplied files, created from compounds with known quantum yields. All UV/vis and PL spectra were recorded at room temperature. The NLO response of the lead iodide-based compounds has been measured using Z-scan[35] and OKE[36] techniques. For the needs of this study, 35 ps and 4 ns laser pulses were used, delivered by a mode-locked Nd:YAG and a Q-switched Nd:YAG laser, respectively, both operating at 10 Hz. The measurements were performed both in the infrared (1064 nm) and in the visible (532 nm). The spot size of the laser beam at the focus (i.e., the beam waist $w_0$ at the focal plane) was 18 $\mu$m at 532 nm and 30 $\mu$m at 1064 nm, for both laser systems.

**Nonlinear Optical Measurements.** Z-scan is a sensitive single-beam technique, based on the measurement of the variation of the transmission of a sample, as the sample is moving along the laser propagation direction ($z$-axis), thus experiencing variable incident intensity levels. The transmitted laser beam is then divided by means of a beam splitter, providing two different experimental configurations. In one part, the so-called "open-aperture" Z-scan (OA), the beam is totally collected by a large diameter lens, allowing the determination of the nonlinear absorption coefficient $\beta$. In the other part, the so-called "closed-aperture" Z-scan (CA), the beam is collected after it passes through a small diameter iris, placed in the far field. From the division of the CA recording by the corresponding OA one, the "divided" Z-scan is obtained, from which the nonlinear refractive index parameter $\gamma'$ can be deduced. The details of the technique have been presented elsewhere.[37] The real and the imaginary part of the third-order susceptibility $\chi^{(3)}$ can be then calculated using the following relations

$$\mathrm{Re}\,\chi^{(3)}\ (\mathrm{esu}) = \frac{c\ (\mathrm{m/s})n_0{}^2\gamma'\ (\mathrm{m}^2/\mathrm{W})}{480\pi^2} \tag{1}$$

$$\mathrm{Im}\,\chi^{(3)}\ (\mathrm{esu}) = \frac{c^2\ (\mathrm{m/s})^2 n_0{}^2\beta\ (\mathrm{m/W})}{960\pi^2\omega\ (\mathrm{s}^{-1})} \tag{2}$$

where $n_0$ is the refractive index of the solvent, $c$ is the speed of light in vacuum, and $\omega$ is the cyclic frequency of the laser pulse. The nonlinar refractive index parameter $\gamma'$ ($m^2/W$) and the nonlinear refractive index $n_2$ (SI) are related through the relation

$$n_2\ (\mathrm{SI}) = \left[\frac{c\ (\mathrm{m/s})n_0\cdot 10^{-8}}{360\pi}\right]\gamma'\ (\mathrm{m}^2/\mathrm{W}) \tag{3}$$

OKE is a pump−probe technique that can provide the third-order susceptibility $\chi^{(3)}$ of a sample, usually measured relatively to a reference material, and its temporal evolution, offering information on the physical mechanisms which are responsible for the observed NLO response. Briefly, the laser beam is split into two parts: a strong (i.e., the pump) and a weak (i.e., the probe) one. The pump beam induces a birefringence in the sample while the probe one is used to detect it. Both beams are linearly polarized, with the polarization of the pump beam being at 45° with respect to the polarization of the probe beam. The two beams, after passing through a Mach−Zehnder interferometer, are focused into the sample by the same lens. One of the arms of the interferometer is equipped with a delay line allowing for the temporal overlapping or delay of the two beams, whereas both beams are spatially overlapped as well, at the focal point, into the sample. The transmitted probe beam becomes elliptically polarized, while in the next it is passing through an analyzer which is set to vertical polarization with respect to the initial probe polarization. Finally, by measuring the probe beam by a photomultiplier, after it has been collected (e.g., by means of a lens), the magnitude of the third-order susceptibility $\chi^{(3)}$ of the sample can be determined through the equation

$$\chi^{(3)}{}_s = \frac{a_s L_s}{e^{-a_s L_s/2}(1 - e^{-a_s L_s})}\left(\frac{I_s}{I_r}\right)^{1/2}\left(\frac{n_s}{n_r}\right)\frac{L_r}{L_s}\chi^{(3)}{}_r \tag{4}$$

where the subscripts $r$ and $s$ are referring to the sample and the reference material, respectively, $I$ is the OKE signal, $\alpha$ is the linear absorption coefficient of the sample, and $L$ is the interaction length of the laser beam with the material. The corresponding second hyperpolarizability $\gamma$ (i.e., the polarizability per molecule) can be obtained by the relation[37]

$$\gamma = \frac{\chi^{(3)}}{NL^4} \tag{5}$$

where $N$ is the number of molecules per unit volume and $L$ is the local field correction factor given by

$$L = \frac{n_0{}^2 + 2}{3} \tag{6}$$

In addition, by varying the time delay between the pump and probe beams, the time evolution of the third-order susceptibility $\chi^{(3)}$ of the sample can be obtained.

## 3. RESULTS AND DISCUSSION

**Characterization.** Structural information for the starting compound has been gained by involving powder XRD methods as well as UV−vis optical absorption and PL spectroscopic methods. In Figure 1, the powder XRD spectrum of a


dx.doi.org/10.1021/jp409620w | J. Phys. Chem. C XXXX, XXX, XXX−XXX

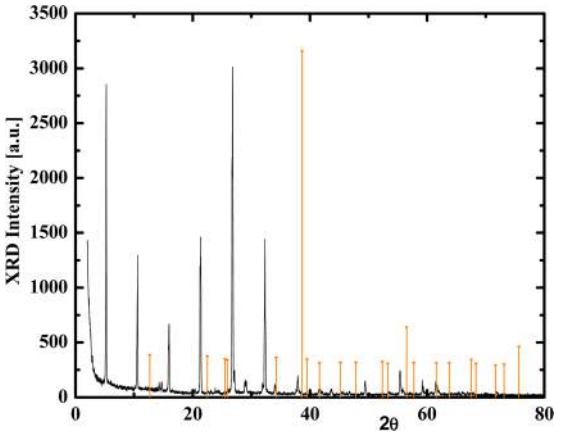


**Figure 1.** Powder XRD spectrum of polycrystalline sample $(FpAH)_2PbI_4$. Red bars indicate the positions of $PbI_2$.

polycrystalline sample of $(FpAH)_2PbI_4$ is shown. Red bars indicate the powder XRD peak positions of $PbI_2$, where it is clear that the starting hybrid compound synthesized has no $PbI_2$ phases. Indexing the XRD peaks by TREOR90 program along with Pawley refinement gives a possible solution to the unit cell structure with *P*4 space group and $a$ = 4.211 Å, $b$ = 4.211 Å, and $c$ = 16.34 Å, while a slightly different synthetic route involving faster cooling, provided crystals with an XRD pattern which can be well fitted with *P*12/*m*1, $a$ = 16.513 Å, $b$ = 8.644 Å, $c$ = 8.186 Å, and $\beta$ = 94.00°, which are close to the reported values given by Mitzi et al. and others[28,29] for similar systems. The slight variation in the lattice constant values is rather usual for this set of organic−inorganic hybrid compounds (i.e., slight structural differences) due to the forces that lead to their formation. In particular, these structural changes are closely related to the position of the $NH_3$ headgroup of each organic molecule, which is being shared by more than one octahedron, as it can be observed in Scheme 1. Also, the tetragonal XRD space group solution appears to provide a unit cell which has half the unit cell along the inorganic layer, probably due to better alignment of the 2D layer octahedrons. In all various synthetic routes for the 2D material, the solid material optical absorption spectra have only slight differences in the peak position and form. Also, no differences are observed when the spectra are obtained from materials recrystallized from AcN solutions.

Figure 2a shows the absorption spectrum of the same material QD solution in AcN. It can be observed that there is a strong absorbance peak at 365 nm, which is also evident in the spectrum of Figures 2b and 2c and is characteristic of lead iodide QDs and more specifically of an isolated lead iodide octahedron. In the particular solutions that are being reported here, the existence of amine salt leads to no evident 2D like micro- or nanosized particles due to the loss of the 512 nm peak. Figure 2b shows the optical absorption spectra of thin deposits of $(FpAH)_2PbI_4$ where it can be clearly seen the excitonic peak at 512 nm and an onset of the energy gap at about 468 nm, leading to an excitonic binding energy of at least 227 meV, quite large due to the dielectric enhancement effect leading to the intense, sharp and distinct excitonic peak. Figure 2c shows the UV−vis absorption spectrum of the 2D material in suspension, formed by diluting AcN solution in HPLC quality $CCl_4$. It can be seen that the peak due to the free 2D exciton appears at 520 nm, probably due to the different structural configuration of the recrystallized material in the suspension or due to some solvent effect. The 0D solutions and the 2D suspensions were constantly checked spectrophotometrically prior to and after laser irradiation to check for their stability. For the needs of the OKE measurements, spectrophotometric grade toluene was used as reference material.

In addition, Figure 3 shows the PL spectra for the 2D solid material, where it is observed that the PL peak, with excitation at 300 nm, appears at 526.5 nm, a Stokes shift of 18 nm. It should be mentioned that in some cases a small second peak, ca. 546 nm, appears in both the absorption and luminescence spectra, probably corresponding to either oxidazed species, inducing trapped excitons. Such an example has been incorporated in Figure 3. The PL spectrum, not shown in this work of the named compound in AcN, shows no peak, close to or above 512 nm, even with excitation higher than the 365 nm absorption peak position.

Finally, it is important to note that the UV−vis absorption of the NLO irradiated samples, as well as of fresh samples, has been monitored with time in the UV−vis optical range to determine the stability of materials. The 0D solutions were

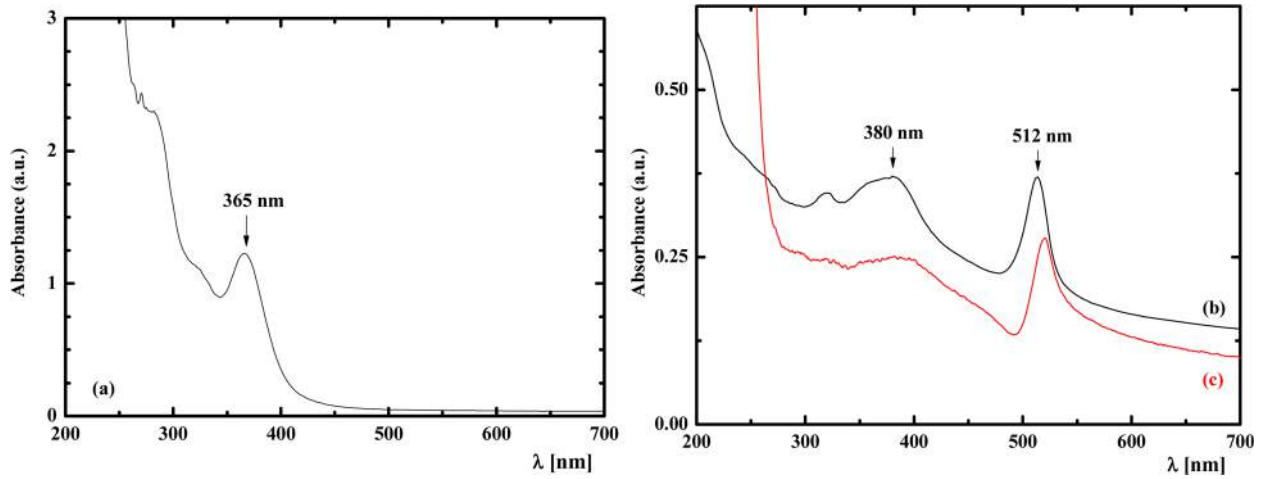


**Figure 2.** Optical absorption spectra: (a) 1.85 mM solution of $PbI_6$-based QDs in AcN, (b) thin deposits of $(FpAH)_2PbI_4$ on quartz substrate, and (c) $(FpAH)_2PbI_4$ 0.2 mM suspension in $CCl_4$, obtained at room temperature.


dx.doi.org/10.1021/jp409620w | J. Phys. Chem. C XXXX, XXX, XXX−XXX

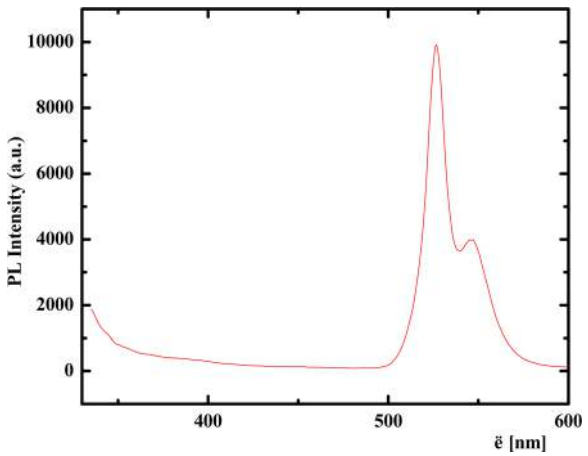


**Figure 3.** Photoluminescence spectrum of a thin deposit of $(FpAH)_2PbI_4$ compound on quartz substrate at room temperature ($\lambda_{exc}$ at 300 nm).

found to be absolutely stable in the range of 2 days, while the 2D suspensions have a shorter life, in terms of the intensity of the excitonic peak at ca. 520 nm, not, however, of the excitonic peak position. This happens probably due to the choice of the fluorophenethylamine and the fact that $CCl_4$ may well dettach the fluorinated organic molecule. Moreover, the suspensions are expected to change in time, since larger species would tend to precipitate. In particular, under still conditions, the excitonic peak position is unchanged for at least a day, while the excitonic optical absorption peak falls by a factor of 2 after 4 h and by 2.5 after 8 h. However, during NLO measurements the suspension has been vigorously stirred every 10 min, thus shifting nanocrystallites in the active region of the solutions. In all cases, some 2D nanocrystallites may have deteriorated in the course of the Z-scan, leading to reduced calculation of the second hyperpolarizability $\gamma$.

**Nonlinear Optical Properties.** For the investigation of the nonlinear optical properties of the samples, several concentration solutions in AcN and suspensions in $CCl_4$ have been prepared, while in order to account for any contribution arising from the solvents, separate measurements of them were performed, under the experimental conditions employed through this work. It is important to note that the concentration of the QDs refers to the concentration of the $(PbI_6)^{4-}$ structural units, while that of the $(FpAH)_2PbI_4$ material refers to the number of octahedra, however, not stand-alone but in corner-sharing configuration. Consequently, the concentration of the active 2D nanoplatelets, formed in the suspension, is at least 16 times less than the reported 2D concentration, although a better minimum bound would be 48 times less, since it needs at least 4 by 4 joined octahedra to form one layer, while 3 layers are needed to form a "sandwich-type" organic−inorganic material behaving as the 2D extended material.

In Figure 4a, some representative divided Z-scans of a 3.12 mM solution of $PbI_6$ in AcN and of neat AcN are presented, both obtained using 3 $\mu$J (i.e., 18.3 GW/cm$^2$), 532 nm, 35 ps laser excitation. As shown, AcN exhibited a valley−peak transmission configuration, indicating positive nonlinear refraction (i.e., $\gamma'$ or $\mathrm{Re}\chi^{(3)} > 0$), while the corresponding divided Z-scan of the solution was found to exhibit similar transmission configuration, but with smaller $\Delta T_{p\text{-}v}$ value than that of the solvent, indicating the opposite sign nonlinear refraction of the solute. That is, $PbI_6$ exhibits negative nonlinear refraction. Similar measurements of the amine salt diluted in AcN, which were performed under identical experimental conditions, have confirmed that the amine salt did not have any contribution to the NLO response of the solutions. Moreover, since the corresponding OA Z-scans of neat AcN, amine salt in AcN and $PbI_6$ solutions in AcN did not exhibit any measurable nonlinear absorption, it can be concluded that the NLO response of the 0D QDs is entirely due to their nonlinear refraction.

The dependence of the $\Delta T_{p\text{-}v}$ parameter of the various $PbI_6$ solutions on the incident laser energy is presented in Figure 5a, the straight lines corresponding to the linear best fits of the experimental data points. As can be seen from this plot, a good linear correlation holds between the values of the $\Delta T_{p\text{-}v}$ parameter and the laser energy in all cases, while the slopes of the straight lines are decreasing with increasing $PbI_6$ concentration, due to the opposite sign refractive nonlinearities of the solvent and the solute. The third-order susceptibility, $\chi^{(3)}$, of AcN determined by the Z-scan technique was found to be $(0.42 \pm 0.02) \times 10^{-13}$ esu, in good agreement with the value of $0.29 \times 10^{-13}$ esu obtained from OKE measurements, under 532 nm, 9 ps laser pulses reported by Ho et al.[36]

Similar Z-scan measurements performed under infrared (i.e., 1064 nm), 35 ps laser excitation and have revealed an identical but weaker NLO response to that found under visible excitation, for both the $PbI_6$ and the AcN. So, negligible NLO absorption and significant NLO refraction have been observed, the solvent exhibiting positive and the $PbI_6$ negative

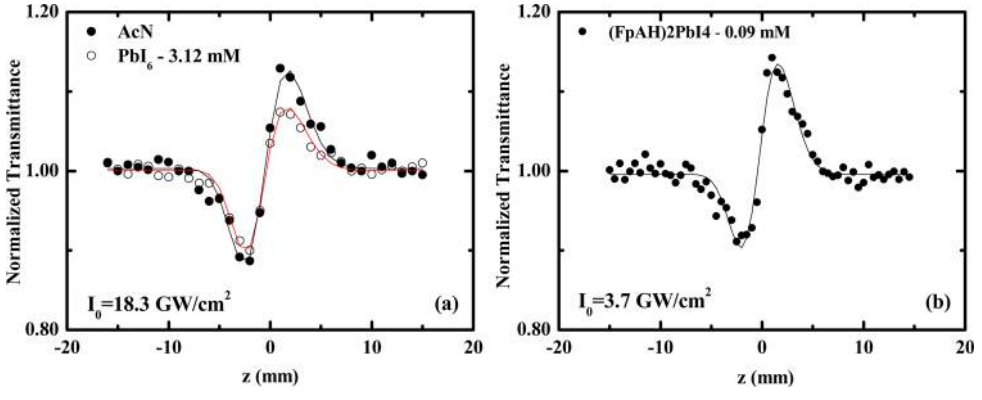


**Figure 4.** Divided Z-scans of (a) a 3.12 mM $PbI_6$ solution and (b) a 0.19 mM $(FpAH)_2PbI_4$ suspension, both obtained under 532 nm, 35 ps.


dx.doi.org/10.1021/jp409620w | J. Phys. Chem. C XXXX, XXX, XXX−XXX

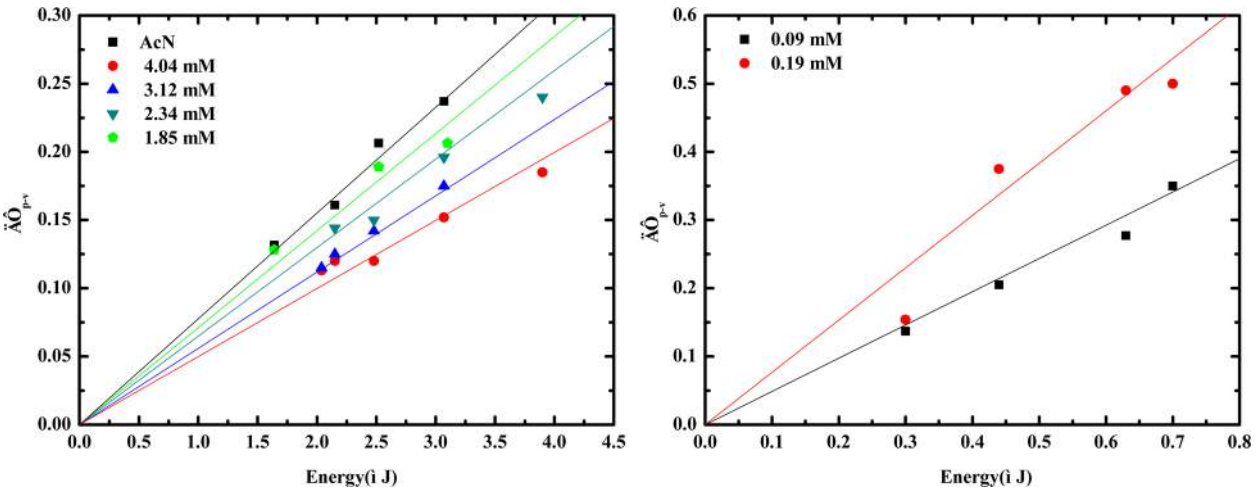


**Figure 5.** Variation of $\Delta T_{p\text{-}v}$ as a function of the incident laser energy for various (a) $PbI_6$ and (b) $(FpAH)_2PbI_4$ concentrations (Z-scan, 532 nm, 35 ps).

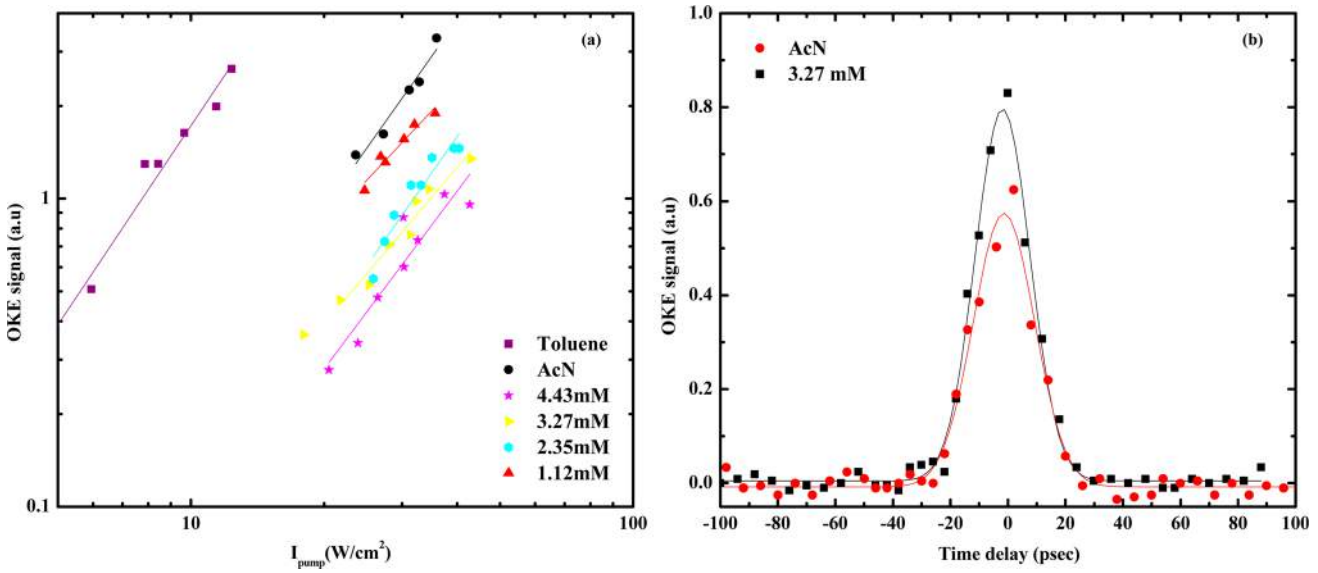


**Figure 6.** (a) Intensity dependence of the OKE signal of various $PbI_6$ concentrations. The OKE signals of the reference material toluene are also included for comparison (35 ps, 532 nm) and (b) time evolution of the OKE signal of a 3.27 mM $PbI_6$ solution and AcN.

nonlinear refraction, respectively. From these measurements, the third-order susceptibility, $\chi^{(3)}$, of AcN was determined to be $(0.22 \pm 0.03) \times 10^{-13}$ esu at 1064 nm and has been taken into account for the determination of the third-order susceptibility, $\chi^{(3)}$, of $PbI_6$ QDs.

In addition to the Z-scan investigation, measurements by the OKE technique were also performed in order to gain insight about the temporal evolution of the optical nonlinearity and for the determination of the magnitude of $\chi^{(3)}$ of the $PbI_6$ QDs, for comparison purposes with the Z-scan results. The OKE measurements were performed with 532 nm, 35 ps laser excitation conditions. In Figure 6a, the intensity dependence of the OKE signal of some $PbI_6$ solutions in AcN is depicted, together with that of (neat) AcN and toluene, the latter used for calibarion purposes. As shown, all OKE signals were found exhibiting a quadratic dependence with the incident pump laser intensity, as expected for third-order nonlinear processes.[36] From these measurements, the $\chi^{(3)}$ value of toluene was found to be $(1.8 \pm 0.25) \times 10^{-13}$ esu, in very good agreement with the $2.38 \times 10^{-13}$ esu value reported by Ho et al.[36] Then, using toluene as reference, the $\chi^{(3)}$ value of AcN was determined to be $(0.29 \pm 0.03) \times 10^{-13}$ esu, which is also in good agreement with the absolute measurement reported above by Z-scan. Considering the contribution of AcN, to the solutions' response, the third-order susceptibility, $\chi^{(3)}$, and the second hyperpolarizability, $\gamma$, values of the $PbI_6$ QDs were obtained and are presented in Table 1. As presented, the $PbI_6$ QDs were exhibited negligible NLO absorption but sizeable, negative sign NLO refraction, both under 35 ps, visible and infrared laser pulses. In addition, their response in the visible was found to be significantly larger than in the infrared, a situation which can be understood by considering two-photon resonant enhancement, which is possible to occur under intense 532 nm laser irradiation, taking also into account the intense bands of the absorption spectrum at about 260 nm in the UV spectral region (see e.g. Figure 2a). A similar resonant enhancement under 1064 nm laser excitation would be significantly less probable, since in this case, four photons would be required for resonant enhancement, the cross section of such process being dramatically lower than a two-photon process. The very good


dx.doi.org/10.1021/jp409620w | J. Phys. Chem. C XXXX, XXX, XXX−XXX

**Table 1. Nonlinear Optical Parameters of the Quantum Dots and Wells Obtained under 35 ps[a]**

| sample | method | $\lambda$ (nm) | $[(PbI_6)^{4-}]$ mM | $\gamma'$ ($\times 10^{-20}$ $m^2/W$) | $n_2$ ($\times 10^{-23}$ $m^2/V^2$) | $\chi^{(3)}$ ($\times 10^{-15}$ esu) | $\gamma$ ($\times 10^{-34}$ esu) |
|---|---|---|---|---|---|---|---|
| $PbI_6$ (0D) | Z-scan | 532 | 4.0 | −10.0 ± 0.6 | −35.6 ± 4.2 | 11.8 ± 0.7 | 19.3 ± 2.2 |
| | | | 3.6 | −9.1 ± 2.0 | −32.3 ± 7.1 | 10.4 ± 2.3 | |
| | | | 2.3 | −6.6 ± 2.0 | −23.4 ± 7.1 | 7.6 ± 2.3 | |
| | | | 1.8 | −5.5 ± 1.0 | −19.5 ± 3.6 | 6.3 ± 1.1 | |
| | | 1064 | 13 | −1.4 ± 0.2 | −5.0 ± 0.7 | 1.6 ± 0.2 | 0.7 ± 0.1 |
| | | | 10 | −0.8 ± 0.2 | −2.9 ± 0.7 | 1.0 ± 0.2 | |
| | | | 7.0 | −0.7 ± 0.1 | −2.4 ± 0.3 | 0.8 ± 0.2 | |
| | | | 4.5 | −0.4 ± 0.1 | −1.4 ± 0.3 | 0.4 ± 0.1 | |
| | OKE | 532 | 4.4 | | | 8.6 ± 0.2 | 13.1 ± 1.0 |
| | | | 3.3 | | | 7.4 ± 0.2 | |
| | | | 2.4 | | | 3.5 ± 0.1 | |
| | | | 1.1 | | | 0.9 ± 0.1 | |
| sample | method | $\lambda$ (nm) | $[FpAH_2PbI_4]$ mM | $\gamma'$ ($\times 10^{-21}$ $m^2/W$) | $n_2$ ($\times 10^{-23}$ $m^2/V^2$) | $\chi^{(3)}$ ($\times 10^{-16}$ esu) | $\gamma$ ($\times 10^{-30}$ esu) |
| $(FpAH)_2PbI_4$ (2D) | Z-scan | 532 | 0.19 | −49.3 ± 4.2 | −175.3 ± 14.9 | 66.3 ± 5.1 | 17.4 ± 1.6 |
| | | | 0.09 | −29.2 ± 2.1 | −103.8 ± 7.4 | 39.4 ± 2.8 | |
| | Z-scan | 1064 | 0.19 | −4.0 ± 1.3 | −14.2 ± 4.6 | 5.0 ± 1.8 | 0.1 ± 0.02 |
| | | | 0.09 | −2.5 ± 0.2 | −8.9 ± 0.7 | 3.3 ± 0.3 | |

[a]The concentration of the active 2D units, however, is at least 16 times less than shown.

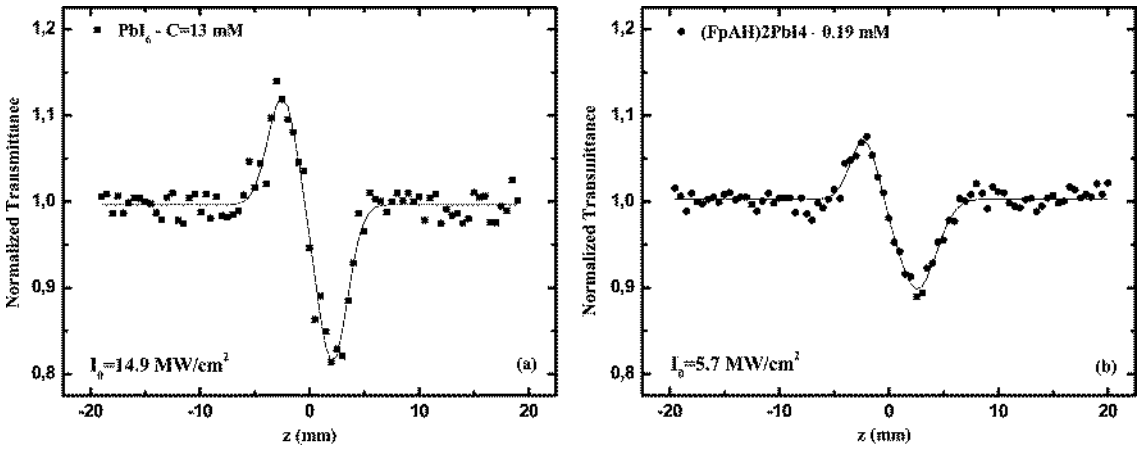


**Figure 7.** Divided Z-scans of (a) a 3.12 mM $PbI_6$ solution and (b) a 0.19 mM $(FpAH)_2PbI_4$ suspension, both obtained under 532 nm, 4 ns.

agreement of the $\chi^{(3)}$ values of the $PbI_6$ QDs, as determined by OKE and Z-scan techniques, has also to be mentioned.

The time dependence of the NLO response of the $PbI_6$ QDs was also studied by OKE for various time delays between the pump and the probe laser beams. In Figure 6b, the dependence of the OKE signals of a 3.27 mM AcN solution of $PbI_6$ and of neat AcN is depicted as a function of the time delay between the pump and the probe beams. In both cases, the response was found to be limited by the laser pulse duration, suggesting that the physical mechanisms responsible for the observed response should be at least faster than the laser pulse duration. Moreover, the solution's OKE signal was found to be smaller than that of solvent, confirming the Z-scan finding, where $PbI_6$ and AcN exhibited opposite sign nonlinear refraction.

The NLO properties of the $(FpAH)_2PbI_4$ suspensions in $CCl_4$, i.e. the 2D material, were investigated under 532 and 1064 nm, 35 ps laser excitation by means of the Z-scan technique. Interestingly, the $(FpAH)_2PbI_4$ suspensions were found exhibiting positive nonlinear refraction (i.e., self-focusing), as suggested by the transmission configuration of the divided Z-scan of a 0.09 mM suspension of Figure 4b and negligible nonlinear absorption. Moreover, since the laser intensity required for the measurements of the suspensions was much lower than that previously needed for the $PbI_6$ measurements, no contribution arising from the solvent was found. In fact, for incident laser intensities as high as 230 GW/$cm^2$, the NLO response of the 2D material was due only to nonlinear refraction. Figure 5b presents the variation of the $\Delta T_{p-v}$ parameter of two $(FpAH)_2PbI_4$ suspensions as a function of the incident laser energy. As shown, in both cases, a linear correlation was found to hold, while from the slopes of the straight lines of Figure 5b, corresponding to the linear best fits of the experimental data points, the nonlinear refractive index parameter $\gamma'$ (i.e., $Re\chi^{(3)}$) of the 2D material has been determined. Taking into account that the concentration of the $(FpAH)_2PbI_4$ in the suspensions was 10−20 times lower than that of the $PbI_6$ QDs and that this concentration refers to each layer, as mentioned before, the present results suggest that the 2D material possess much higher optical nonlinearity than its building blocks (i.e., $(PbI_6)^{4-}$). In fact, since the active units in the suspension of the 2D material are at least 16 times less than the sample's molarity, the nonlinear refractive index $\gamma'$ or the third-order susceptibility $\chi^{(3)}$ (since there is no nonlinear absorption) would be at least 16 times larger than those reported in Table 1. The dielectric enhancement effect, the Bohr radius, and the coherence length of the exciton within the


dx.doi.org/10.1021/jp409620w | J. Phys. Chem. C XXXX, XXX, XXX−XXX

Table 2. Nonlinear Optical Parameters of the Quantum Dots and Wells Obtained under 4 ns, 532 nm

| sample | $[(PbI_6)^{4-}]$ mM | $\gamma'$ ($\times 10^{-20}$ $m^2/W$) | $n_2$ ($\times 10^{-21}$ $m^2/V^2$) | $\chi^{(3)}$ ($\times 10^{-15}$ esu) | $\gamma$ ($\times 10^{-32}$ esu) |
|---|---|---|---|---|---|
| $PbI_6$ (0D) | 9.1 | −480 ± 110 | 17.1 ± 3.9 | 550 ± 130 | 2.2 ± 0.5 |
| | 6.3 | −356 ± 48 | 12.7 ± 1.7 | 405 ± 54 | |
| | 3.7 | −252 ± 62 | 9.0 ± 2.2 | 287 ± 70 | |
| sample | [ $FpAH_2PbI_4$] mM | $\gamma'$ ($\times 10^{-20}$ $m^2/W$) | $n_2$ ($\times 10^{-21}$ $m^2/V^2$) | $\chi^{(3)}$ ($\times 10^{-15}$ esu) | $\gamma$ ($\times 10^{-28}$ esu) |
| $(FpAH)_2PbI_4$ (2D) | 0.19 | −37 ± 8 | 1.3 ± 0.2 | 50 ± 11 | 1.2 ± 0.1 |
| | 0.09 | −17 ± 5 | 0.6 ± 0.1 | 23 ± 7 | |

2D layered system as well as the coherence length of the exciton within the microdroplet of AcN within the suspension, which may contain more than one 2D nanocrystallite, give rise to this intense NLO response, as already predicted by Hanamura.[38,39] An important fact leading to intense NLO activity could be the critical range of the micelle's nanocrystals at which energy trasnfer effects take place, leading to superluminescence.[40] In addition to the above, the spectral position of the characteristic band of the 2D material lying at 512 nm (see e.g. absorption spectrum of Figure 2b) which is almost resonant with the excitation wavelength, is expected to contribute efficiently to the impressively higher second hyperpolarizability $\gamma$ values determined here (see e.g. Table 1).

Finally, the NLO properties of the lead iodide-based systems (i.e., $PbI_6$ and $(FpAH)_2PbI_4$) were further investigated under 4 ns, 532 and 1064 nm laser excitation, employing the Z-scan technique as well. In this case, under 532 nm laser excitation, both the 0D and the 2D materials were found to exhibit similar NLO response, i.e., negative nonlinear refraction (i.e., peak−valley transmission configuration) and insignificant nonlinear absorption, while the solvents (i.e., AcN and $CCl_4$) did not have any contribution under nanosecond excitation. Some typical "divided" Z-scans of a 13 mM $PbI_6$ solution and a 0.19 mM $(FpAH)_2PbI_4$ suspension are shown in Figures 7a and 7b, respectively, showing peak−valley transmission configuration, indicating negative nonlinear refraction ($Re\chi^{(3)}$), corresponding to self-defocusing behavior. Similar measurements with 1064 nm laser excitation did not show any measurable NLO response for incident intensities up to 300 $MW/cm^2$. The NLO paremeters obtained under 4 ns are included in Table 2.

Athough the NLO response of several 0D and 2D semiconducting structures has been extensively studied in the past, there are no reports concerning the NLO properties of $Pb_xI_y$-based 0D and 2D materials, to the best of our knowledge. In that sense, only an indirect comparison can be made between the present findings and other literature reports, since different types of semiconducting QDs exhibit different NLO behavior based on their size and exciton binding energy. The most studied QDs are the CdSeS,[12] CdS,[41] or CdSe/ZnS.[42,43] These systems tend to exhibit strong reverse saturable absorption behavior, attributed to free carrier absorption. Nevertheless, the class of hybrid organic−inorganic materials studied in the present study was found to exhibit insignificant nonlinear absorption and strong nonlinear refraction, under all the experimental conditions employed, suggesting that these materials could be promising candidates for several applications in optoelectronics where absorption is unwanted. In addition, and maybe most important, is the large enhancement of the NLO response found for the 2D material where an almost 5 orders of magnitude higher second hyperpolarizability $\gamma$ values were obtained compared to the corresponding $PbI_6$ 0D material.

Hanamura et al.[44] were the first to examine (theoretically) the possibility of modulating the third-order NLO response of semiconducting quantum wells sandwiched by barriers with lower dielectric constant and larger energy gap owing to the increase of the exciton binding energy. In addition, other studies[38,39,45] have shown that the nanocrystal particle size strongly affects the excitonic oscillator strength and consequently the optical nonlinearity of the QDs, besides the effect of dense excitonic population leading to the dielectric constant change.[18,19] In particular, concerning the lead iodide-based structures, Ishihara et al.[46,47] based on the previously mentioned studies showed that the 10 Å thick layered perovskite $(C_{10}H_{21}NH_3)_2PbI_4$ material exhibits extremely large binding energy and oscillator strength, ensuing strongly enhanced NLO response. On the basis of these studies, Xu and co-workers[14] have determined the $\chi^{(3)}$ of the 2D material, i.e., $(C_{10}H_{21}NH_3)_2PbI_4$, with its excitonic peak located at 511.8 nm, by means of third-harmonic generation (THG) in the 1.5−1.7 $\mu$m range. A clear enhancement of the $\chi^{(3)}$ has been reported at 1.5 $\mu$m due to three-photon resonance enhancement, and monotonic reduction of the $\chi^{(3)}$ was observed as the excitation wavelength was shifted far from 1.5 $\mu$m, evidencing the strong influence of the position of the excitonic peak on the NLO properties of such materials. The $\chi^{(3)}$ value obtained at 1.53 $\mu$m was reported to be of the order of $10^{-9}$ esu. Also, it should be taken into consideration that the octahedrals are mainly interacting among them and less with amine, unlike the isolated $PbI_6$ QDs of this work, which are interacting basically with the amine which stabilizes them.

## 4. CONCLUSIONS

Synthesis and nonlinear study are reported on hybrid organic inorganic LD lead iodide-based QDs and suspensions, in particular based on $(PbI_6)^{4-}$ structural units as stand-alone for the QDs or as corner-sharing for the 2D. The suspension's micelles contain 2D hybrid organic−inorganic nanocrystals, possibly in sustainable energy transfer proximity within each micelle. The 2D semiconductor material and the 0D $(PbI_6)^{4-}$ QDs were characterized by X-ray diffraction, UV−vis absorption, and PL/PLE spectroscopy, revealing the excitonic peak of the first at 512 nm, typical of lead iodide 2D materials and the characteristic absorption peak of the QD at 365 nm, typical of isolated lead iodide octahedra. Furthermore, NLO measurements of the 0D and 2D materials were conducted, employing Z-scan and OKE techniques, under 35 ps laser excitation, while the transient NLO response was also examined using 4 ns laser pulses. The two materials were found to exhibit strong nonlinear refraction and insignificant nonlinear absorption. However, the resonant conditions met in the case of the 2D material gave rise to an unprecedented enhancement of the NLO response compared to the 0D material, for both picosecond and nanosecond laser excitation. To the best of our knowledge, this is the first time that the third-order NLO


dx.doi.org/10.1021/jp409620w | J. Phys. Chem. C XXXX, XXX, XXX−XXX

response of such lead iodide-based semiconductors is being reported in detail.

## AUTHOR INFORMATION


### Corresponding Authors

*E-mail ikouts@upatras.gr (I.K.).
*E-mail couris@iceht.forth.gr (S.C.).


### Notes

The authors declare no competing financial interest.

## ACKNOWLEDGMENTS

I.P. and S.C. acknowledge partial support by the European Union (European Social Fund−ESF) and Greek national funds through the Operational Program "Education and Lifelong Learning" of the National Strategic Reference Framework (NSRF)-Research Funding Programs: Heracleitus II and THALIS: Investing in knowledge society through the European Social Fund.

## REFERENCES


(1) Srinivasan, K.; Painter, O. Linear and Nonlinear Optical Spectroscopy of a Strongly Coupled Microdisk−Quantum Dot System. *Nature* **2007**, *450*, 862−866.

(2) Kondo, T.; Azuma, T.; Yuasa, T.; Ito, R. Biexciton Lasing in the Layered Perovskite-Type Material $(C_6H_{13}NH_3)_2PbI_4$. *Solid State Commun.* **1997**, *105*, 253−255.

(3) Flatte, M. E.; Kornyshevb, A. A.; Urbakh, M. Giant Stark Effect in Quantum Dots at Liquid/Liquid Interfaces: A New Option for Tunable Optical Filters. *Proc. Natl. Acad. Sci. U. S. A.* **2008**, *105*, 18212−18214.

(4) Chakravarthy, V.; Guloy, A. M. Synthesis and Structure of a New Layered Organic−Inorganic Compound Containing Unique Chains of $PbI_2$. *Chem. Commun.* **1997**, 697−698.

(5) Devic, T.; Canadell, E.; Auban-Senzier, P.; Batail, P. $(EDT\text{-}TTF\text{-}I_2)_2PbI_3{\cdot}H_2O$: an Ambient Pressure Metal with a b′ Donor Slab Topology. *J. Mater. Chem.* **2004**, *14*, 135−137.

(6) Billing, D. G.; Lemmerer, A. Poly[bis[2-(1-cyclohexenyl)-ethylammonium] di-mu-iodo-diodoplumbate(II)]. *Acta Crystallogr., C* **2006**, *62*, 269−271.

(7) Chen, X. B.; Li, H.-H.; Chen, Z.-R.; Liu, J.-B.; Li, J.-B.; Dong, H.-J.; Wu, Y. L. Introducing Transition-Metal Complex Together with Conjugated Ligand into Polymeric Iodoplumbate: Structure Characterization, Properties and Theoretical Study of a New Semi-Conductive Hybrid: $\{[Cu(II)(2,2'\text{-bipy})_3][Pb_2I_6]\}_n$. *J. Cluster Sci.* **2009**, *20*, 611−620.

(8) Karabulut, I.; Baskoutas, S. Linear and Nonlinear Optical Absorption Coefficients and Refractive Index Changes in Spherical Quantum Dots: Effects of Impurities, Electric Field, Size, and Optical Intensity. *J. Appl. Phys.* **2008**, *103*, 073512.

(9) Karabulut, I.; Safak, H.; Tomak, M. Excitonic Effects on the Nonlinear Optical Properties of Small Quantum Dots. *J. Appl. Phys. D: Appl. Phys.* **2008**, *41*, 155104.

(10) Shi, W.; Chen, Z.; Liu, N.; Lu, H.; Zhou, Y.; Cui, D.; Yang, G. Nonlinear Optical Properties of Self-Organized Complex Oxide $Ce:BaTiO_3$ Quantum Dots Grown by Pulsed Laser Deposition. *Appl. Phys. Lett.* **1999**, *75*, 1547−1549.

(11) Kondo, T.; Iwamoto, S.; Hayase, S.; Tanaka, K.; Ishi, J.; Mizuno, M.; Ema, K.; Ito, R. Resonant Third-Order Optical Nonlinearity in the Layered Perovskite-Type Material $(C_6H_{13}NH_3)_2PbI_4$. *Solid State Commun.* **1998**, *105*, 503−506.

(12) Wu, F.; Zhang, G.; Tian, W.; Ma, L.; Chen, W.; Zhao, G.; Cao, S.; Xie, W. Nonlinear Optical Properties of $CdSe_{0.8}S_{0.2}$ Quantum Dots. *J. Opt. A: Pure Appl. Opt.* **2008**, *10*, 075103.

(13) Shimizu, M.; Fujisawa, J.-I.; Ishihara, T. Photoluminescence of the Inorganic-Organic Layered Semiconductor $(C_6H_5C_2H_4NH_3)_2PbI_4$: Observation of Triexciton Formation. *Phys. Rev. B* **2006**, *74*, 155206.

(14) Xu, C.-q.; Kondo, T.; Sakakura, H.; Kumata, K.; Takahashi, Y.; Ito, R. Optical Third-Harmonic Generation in Layered Perovskite-Type Material $(C_{10}H_{21}NH_3)_2PbI_4$. *Solid State Commun.* **1991**, *79*, 245−248.

(15) Kato, Y.; Ichii, D.; Ohashi, K.; Kunugita, H.; Ema, K.; Tanaka, K.; Takahashi, T.; Kondo, T. Extremely Large Binding Energy of Biexcitons in an Organic-Inorganic Quantum-Well Material $(C_4H_9NH_3)_2PbBr_4$. *Solid State Commun.* **2003**, *128*, 15−18.

(16) Kitazawa, N. Preparation and Optical Properties of Nanocrystalline $(C_6H_5C_2H_4NH_3)_2PbI_4$-Doped PMMA Films. *J. Mater. Sci.* **1998**, *33*, 1441−1444.

(17) Zhang, S.; Lanty, G.; Lauret, J.-S.; Deleporte, E.; Audebert, P.; Galmiche, L. Synthesis and Optical Properties of Novel Organic-Inorganic Hybrid Nanolayer Structure Semiconductors. *Acta Mater.* **2009**, *57*, 3301−3309.

(18) Ishihara, T. Optical Response of Semiconductor and Metal-Embedded Photonic Crystal Slabs. *Phys. Status Solidi A* **2004**, *201*, 398−404.

(19) Kondo, T.; Xu, C.-Q.; Ito, R. *Linear and Nonlinear Optical Properties of a Natural Quantum-Well Material* $(C_{10}H_{21}NH_3)_2PbI_4$; Elsevier: Amsterdam, 1992.

(20) Troles, J.; Smektala, F.; Boudebs, G.; Monteil, A. Third-Order Nonlinear Optical Characterization of New Chalcohalogenide Glasses Containing Lead Iodine. *Opt. Mater.* **2003**, *22*, 335−343.

(21) Papavassiliou, G. C. Three and Low-Dimensional Inorganic Semiconductors. *Prog. Solid State Chem.* **1997**, *25*, 125−270.

(22) Takada, T.; Mackenzie, J. D.; Yamane, M.; Kang, K.; Peyghambarian, N.; Reeves, R. J.; Knobbe, E. T.; Powell, R. C. Preparation and Non-Linear Optical Properties of CdS Quantum Dots in $Na_2O\text{-}B_2O_3\text{-}SiO_2$ Glasses by the Sol Gel Technique. *J. Mater. Sci.* **1996**, *31*, 423−430.

(23) Chowdhury, S.; Hussain, A. M. P.; Ahmed, G. A.; Mohanta, D.; Choudhury, A. Third Order Nonlinear Optical Response of PbS Quantum Dots. *Semicond. Phys., Quantum Electron. Optoelectron.* **2006**, *9*, 45−48.

(24) Uhrig, A.; Wörner, A.; Klingshirn, C.; Banyai, L.; Gaponenko, S.; Lacis, I.; Neuroth, N.; Speit, B.; Remitz, K. Nonlinear Optical Properties of Semiconductor Quantum Dots. *J. Cryst. Growth* **1992**, *117*, 598−602.

(25) Horan, P.; Blau, W.; Byrne, H.; Berglund, P. Simple Setup for Rapid Testing of Third-Order Nonlinear Optical Materials. *Appl. Opt.* **1990**, *29*, 31−36.

(26) Jiao, Y.; Yu, D.; Wang, Z.; Tang, K.; Sun, X. Synthesis, Nonlinear Optical Properties and Photoluminescence of ZnSe Quantum Dots in Stable Solutions. *Mater. Lett.* **2007**, *61*, 1541−1543.

(27) Dammak, T.; Koubaa, M.; Boukheddaden, K.; Bougzhala, H.; Mlayah, A.; Abid, Y. Two-Dimensional Excitons and Photoluminescence Properties of the Organic/Inorganic $(4\text{-}FC_6H_4C_2H_4NH_3)_2[PbI_4]$ Nanomaterial. *J. Phys. Chem. C* **2009**, *113*, 19305−19309.

(28) Mitzi, D. B.; Dimitrakopoulos, C. D.; Rosner, J.; Medeiros, D. R.; Xu, Z.; Noyan, C. Hybrid Field-Effect Transistor Based on a Low-Temperature Melt-Processed Channel Layer. *Adv. Mater.* **2002**, *14*, 1772−1776.

(29) Mitzi, D. B.; Dimitrakopoulos, C. D.; Kosbar, L. L. Structurally Tailored Organic−Inorganic Perovskites: Optical Properties and Solution-Processed Channel Materials for Thin-Film Transistors. *Chem. Mater.* **2001**, *13*, 3728−3740.

(30) Koutselas, I. B.; Ducasse, L.; Papavassiliou, G. C. Electronic Properties of Three- and Low-Dimensional Semiconducting Materials with Pb Halide and Sn Halide Units. *J. Phys.: Condens. Matter* **1996**, *8*, 1217.

(31) Papavassiliou, G. C.; Koutselas, I. B. Structural, Optical and Related Properties of some Natural 3-Dimensional and Lower-Dimensional Semiconductor Systems. *Synth. Met.* **1995**, *71*, 1713−1714.

(32) Baibarac, M.; Preda, N.; Mihut, L.; Baltog, I.; Lefrant, S.; Mevellec, J. Y. On the Optical Properties of Micro- and Nanometric Size $PbI_2$ Particles. *J. Phys.: Condens. Matter* **2004**, *16*, 2345−2356.

(33) Sandroff, C. J.; Hwang, D. M.; Chung, W. M. Carrier Confinement and Special Crystallite Dimensions in Layered Semiconductor Colloids. *Phys. Rev. B* **1986**, *33*, 5953−5955.
(34) Jones, A. R.; Aikens, D. A. The Nature of Pb(II)-Bromide Complexes in Propylene Carbonate. *Polyhedron* **1982**, *1*, 169−174.
(35) Sheik-Bahae, M.; Said, A. A.; Wei, T. H.; Hagan, D. J.; Van Stylard, E. W. Sensitive Measurement of Optical Nonlinearities Using a Single Beam. *IEEE J. Quantum Electron.*. **1990**, *26*, 760−769.
(36) Ho, P. P.; R. R. Alfano, R. R. Optical Kerr Effect in Liquids. *Phys. Rev. A* **1979**, *20*, 2710−2187.
(37) Couris, S.; Koudoumas, E.; Ruth, A. A.; Leach, S. Concentration and Wavelength Dependence of the Effective Third Order Susceptibility and Optical Limiting of C60 in Toluene. *J. Phys. B: At. Mol. Opt. Phys.* **1995**, *2*, 4537−4554.
(38) Hanamura, E. *Nonlinear Optics in Semiconductors II*; Academic Press: Waltham, MA, 1998.
(39) Hanamura, E. *Optical Switching in Low-Dimensional Solids*; Plenum Press: London, 1988.
(40) Papavassiliou, G. C.; Pagona, G.; Karousis, N.; Mousdis, G. A.; Koutselas, I.; Vassilakopoulou, A. Nanocrystalline/Microcrystalline Materials Based on Lead-Halide Units. *J. Mater. Chem.* **2012**, *22*, 8271−8280.
(41) Liu, X.; LiuAdachi, Y.; Tomita, Y.; Oshima, J.; Nakashima, T.; Kawai, T. High-Order Nonlinear Optical Response of a Polymer Nanocomposite Film Incorporating Semiconducotor CdSe Quantum Dots. *Opt. Express* **2012**, *20*, 13457−13469.
(42) Dneprovskii, V.; Kabanin, D.; Lyaskovskii, V.; Santalov, A.; Wumaier, T.; Dang, T. G.; Zhukov, E. Nonlinear Absorption and Refraction of CdSe/ZnS Quantum Dots at Two-Photon Resonant Excitation of Excitons. *Phys. Status Solidi C* **2008**, *5*, 2507−2510.
(43) Dneprovskii, V.; Kozlova, M.; Smirnov, A.; Wumaier, T. The Features of Nonlinear Absorption of Two-Photon Excited Excitons in CdSe/ZnS Quantum Dots. *Physica E* **2012**, *44*, 1920−1923.
(44) Hanamura, E.; Nagaosa, N.; Kumagai, M.; Takagahara, T. Quantum Wells with Enhanced Exciton Effects and Optical Nonlinearity. *J. Mater. Sci. Eng.* **1988**, *1*, 255.
(45) Takagahara, T. Excitonic Optical Nonlinearity and Exciton Dynamics in Semiconductor Quantum Dots. *Phys. Rev. B* **1987**, *36*, 9293−9296.
(46) Ishihara, T.; Takahashi, J.; Goto, T. Exciton State in Two-Dimensional Perovskite Semiconductor $(C_{10}H_{21}NH_3)_2PbI_4$. *Solid State Commun.* **1989**, *69*, 933.
(47) Ishihara, T.; Takahashi, J.; Goto, T. Optical Properties Due to Electronic Transitions in Two-Dimensional Semiconductors $(C_nH_{2n+1}NH_3)_2PbI_4$. *Phys. Rev. B* **1990**, *42*, 11099.